2016

A MECHANISTIC STUDY OF AN iPSC MODEL FOR LEIGH'S DISEASE CAUSED BY MtDNA MUTATAION (8993 T>G)

John P. Galdun
Virginia Commonwealth University

A MECHANISTIC STUDY OF AN iPSC MODEL FOR LEIGH'S DISEASE CAUSED BY MtDNA MUTATAION (8993 T>G)

A thesis submitted in partial fulfillment of the requirements for the degree of Master of Science at Virginia Commonwealth University

By

John Patrick Galdun III, B.S. (Microbiology)

University of Georgia, 2013

Director: Raj R. Rao

Associate Professor

Department of Chemical and Life Science Engineering

Virginia Commonwealth University

Richmond, Virginia

June, 2016

ACKNOWLEDGEMENTS

I would like express my gratitude to the people who have supported me through the completion of my Masters project. Thank you to the members of the Phyiology and Biophysics department and associates, particularly Dr. Roland Pittman and Ms. Christina Kyrus, for educating me, and guiding me through the necessary steps to complete my degree.

To the members of the Virginia Commonwealth University Nucleic Acids Research Facilities: I would like to thank Dr. Yingping Wang for carrying out Sanger sequencing, Dr. Myrna G. Serrano for assistance with the whole exome next-gen sequencing, and Dr. Vishal N Koparde for sequencing data analysis. This project was heavily dependent upon their hard work, and I am forever grateful for it.

Additionally, I would like to acknowledge my committee members; Dr. Liya Qiao, Dr. Edward Lesnefsky, and Dr. Shilpa Iyer. Thank you for helping me achieve my goal, and providing your time and feedback along the way.

Of course, thank you to everyone in the Rao Lab; Alex Ip and Dr. Venkat S. Gadepalli for your collaboration and guidance. I want to thank my advisor Dr. Raj R. Rao for everything associated with this project and helping me complete my degree. It was a pleasure working with you.

Lastly, I would like to thank my family and friends for their continued moral and financial support. Without you, this would not have been possible.

TABLE OF CONTENTS

LIST OF TABLES

LIST OF FIGURES

LIST OF ABBREVIATIONS

AD	Alzheimer's Disease
ATP	Adenosine Triphosphate
ddC	Dideoxycytidine
ER	Endoplasmic Reticulum
ESC	Embryonic Stem Cell
ETC	Electron Transport Train
hNP	Human Neural Progenitor
IGV	Integrative Genomics Viewer
iPSC	Induced Pluripotent Stem Cell
LHON	Leber's Hereditary Optic Neuropathy
MtDNA	Mitochondrial Deoxyribonucleic Acid
MELAS	Mitochondrial Encephalomyopathy Lactic Acidosis and Stroke like Episodes
MFRTA	Mitochondrial Free Radical Theory of Ageing
MIDD	Maternally Inherited Diabetes and Deafness
MPTP	1-Methyl-4-phenyl-1,2,3,6-tetrahydropyridine
NADH	Nicotinamide Adenine Dinucleotide
NARP	Neurogenic Muscle Weakness, Ataxia, and Retinitis Pigmentosa
PD	Parkinson's Disease

ROS	Reactive Oxygen Species
SAM	Sequence Alignment Map
VCF	Variant Calling File

ABSTRACT

A MECHANISTIC STUDY OF AN iPSC MODEL FOR LEIGH'S DISEASE CAUSED BY MtDNA MUTATAION (8993 T>G)

By, John Patrick Galdun III B.S. (Microbiology) University of Georgia, 2013

A thesis submitted in partial fulfillment of the requirements for the degree of Master of Science at Virginia Commonwealth University.

Virginia Commonwealth University, 2016

Major Director: Raj R. Rao Ph.D, Associate Professor, Department of Chemical and Life Science Engineering

Mitochondrial diseases encompass a broad range of devastating disorders that typically affect tissues with high-energy requirements. These disorders have been difficult to diagnose and research because of the complexity of mitochondrial genetics, and the large variability seen among patient populations. We have devised and carried out a mechanistic study to generate a cell based model for Leigh's disease caused by mitochondrial DNA mutation 8993 T>G. Leigh's

disease is a multi-organ system disorder that depends heavily on the mutation burden seen within various tissues. Using new reprogramming and sequencing technologies, we were able to show that Leigh's disease patient fibroblasts reprogrammed to induced pluripotent stem cells maintain the same level of mutation burden seen in the original patient cell line. Mutation burden was maintained through several passages and spontaneous differentiation. This cell based model could be useful for future pathogenesis studies, or therapeutic drug screenings in a patient and tissue specific manner.

CHAPTER 1: INTRODUCTION

A. Mitochondria Structure, Function, and Genetics

1. Structure

Through DNA sequencing technologies and homology analysis, it is theorized that mitochondria arose from an α −Proteobacterial progenitor that formed an endosymbiotic relationship with an ancestral type of eukaryotic cell (95, 26). As such, mitochondria share a structural resemblance to their prokaryotic ancestors; possessing two separate and functionally unique membranes referred to as the outer membrane and inner membrane (41). The outer membrane separates the mitochondria from the cytoplasm and surrounds the inner membrane. Unlike the inner membrane, the outer membrane is rather porous. Ions and small-uncharged particles are able to flow through membrane protein porins, such as the voltage-dependent anion channel (4). The inner membrane is the site of the protein complexes responsible for generating the electrochemical gradient needed for adenosine triphosphate (ATP) synthesis in oxidative phosphorylation (41). The inner membrane is subdivided into two contiguous regions known as the inner boundary membrane, which lies close to the outer membrane, and the cristae, which are folded invaginations of the inner membrane into the interior of the mitochondrion (60). A large complex of proteins known as the mitochondrial contact site and cristae organizing system is

responsible for upholding the integrity of the folded cristae, and furthermore, maintaining the efficiency of energy production (23, 75, 61).

The two membranes divide the mitochondrion into three compartments that serve different functions, and possess different protein components. The intermembrane space is the compartment between the outer and inner membrane, where much of the transportation machinery resides (56). The innermost compartment of the mitochondrion, the matrix, houses the double stranded circular mitochondrial deoxyribonucleic acid (mtDNA) molecule, as well as serves as the location for numerous enzymatic reactions, mitochondrial transcription, and mitochondrial translation carried out by the mitochondrial ribosomes, or mitoribosomes (81). The cristae delineate the final compartment, which is the cristae lumen. As the cristae membrane is the site for most of the protein complexes of the respiratory chain, the cristae lumen is the location where the proton gradient is formed (41). Complex V, or ATP synthase, is directly responsible for using the energy stored in the electrochemical proton gradient to produce ATP from adenosine diphosphate (ADP) and phosphate (12). Individual ATP synthases are composed of more than 20 individual proteins, and ATP synthases form supramolecular dimers and oligomers in long rows along the strongly curved regions of the cristae membrane (76). These dimers have been shown to be a universal feature among many mitochondria investigated. If certain subunits are removed from ATP synthases, dimers are unable to form, and the mitochondria lack the highly folded cristae that are typical of cristae morphology. From theses studies, it is clear that ATP synthase plays a role in generating the folded mitochondrial cristae. Given the importance of ATP synthase in the electron transport chain (ETC), any alterations in the complex itself or the supramolecular structure it forms could have functional implications on

the efficiency of oxidative phosphorylation and ultimately play a role in pathophysiological conditions (59, 76).

Different tissue and cell types show variability in mitochondrial arrangement and morphology. For instance, neuronal mitochondria are very dynamic and use various cytoskeletal components and specific motor proteins to move to different areas of the cell when needed (71). On the other hand, mitochondria of cardiomyocytes display a regular and fixed intracellular arrangement similar to a crystal (6). Mitochondria can also be found in close association with the endoplasmic reticulum (ER), which has functional implications that are discussed in a later section (66). In addition to variance among cell types, mitochondria can be dynamic in number and morphology within a single cell during times of development, cell cycle stages, or when exposed to stressors. Mitochondria can be long and filamentous, short and rod-like, and under conditions of compromised function, small and spherical (42, 35). Fusion and fission reactions control the number of mitochondria within a cell, and can also control mitochondrial morphology and organization (5). The heterogeneity in these organelles with regards to shape and intercellular arrangement can most often be attributed to the various functions and energy demands required of them by the cell in which they occupy.

2. Function

A recent flourish in mitochondrial research has led to the discovery of additional important mitochondrial functions. As previously stated, the ER has a special membrane domain that interacts with the mitochondria referred to as the mitochondria-associated ER membrane. The proteins and enzymes within this region play important roles in calcium signaling (64). Mitochondrial calcium uptake has been shown to increase ATP production (53, 9), as well as

buffer the cytosolic calcium concentration (67). Regulation of the intracellular calcium concentration is critical for transcriptional regulation, metabolic processes, hormone release, and maintaining cell life or cell death signals (58, 30). Mitochondria also exhibit mechanisms of either inducing or inhibiting apoptosis.

Apoptosis is a process where cells activate an organized cell suicide pathway leading to their breakdown and eventual phagocytosis. This is distinct from necrosis, and displays the morphological characteristics of cell shrinkage, membrane blebbing, and DNA cleavage and separation into apoptotic bodies with cell surface markers bringing about phagocytosis (39). Although additional mechanisms exist, the two most commonly characterized are the death receptor pathway, also known as the extrinsic pathway, and the mitochondrial pathway, also known as the intrinisic pathway. Both pathways ultimately lead to the activation of caspases, cysteine proteases that cleave after aspartate residues, which selectively cleave intracellular components resulting in cell death (65). Numerous cell stresses initiate the mitochondrial pathway including developmental cues, growth factor deprivation, ER stress, and DNA damage (27). The mitochondria respond by releasing the apoptosis inducing cytochrome c, as well as proapoptotic (Bax, Bak) and antiapoptotic (Bcl-2, Bcl-xL) members of the Bcl-2 family. The delicate interplay of these mitochondrial factors results in a controlled activation of caspases leading to apoptosis (48, 96, 21).

Mitochondria also play a key role in maintaining cellular redox potential. In order to establish the electrochemical gradient and generate ATP, a series of redox reactions must take place, wherein electrons pass along a series of enzymes located in the inner membrane causing the release of free energy allowing the proton flux from the matrix to the intermembrane space. The coupling of ATP synthesis to the mitochondrial redox environment remains a topic of

debate. However, these redox reactions leading to oxidative phosphorylation, particularly the reoxidation of nicotinamide adenine dinucleotide (NADH) to NAD+, have clear implications on the mitochondrial redox environment (52). Alterations in the mitochondrial redox environment occur in numerous pathological conditions such as ischemic reperfusion injury and various cancers highlighting the importance of this mitochondrial function (43, 46).

Mitochondria are most noted for their energy producing capabilities. Rightfully so, as on average the human body requires 50 kg of ATP turnover daily and the majority of this ATP is generated by oxidative phosphorylation in the mitochondria (3). The enzyme complexes that comprise the ETC are comprised of multiple subunits that can be encoded for by the nuclear DNA or the mtDNA.

3. Genetics

Almost all of the over 3000 proteins in mitochondria are coded for by nuclear DNA, transcribed, translated by cytosolic ribosomes, and then transported into the mitochondria. Effective nuclear-mitochondria cross talk is absolutely essential for normal mitochondrial function (94). Although nuclear DNA encodes for most of the human mitochondrial proteins, the circular, double stranded, and 16,569 bases in length human mtDNA molecule is responsible for 37 genes including 22 tRNAs, 2 rRNAs, and 13 proteins. Human mtDNA contains very few introns, and is transcribed polycistronically. There are slight differences in the translation code that prevent nuclear DNA from being translated by mitoribosomes and vice versa (74). All 13 proteins encoded for by mtDNA form subunits of ETC complexes, and are essential for normal oxidative phosphorylation.

Mitochondrial genes are not inherited in the same fashion as nuclear genes. There is evidence to suggest that paternal mitochondria are actively tagged for degradation after

fertilization, and thus only the maternal mtDNA is inherited. This is known as a maternal inheritance pattern (33, 80). The complete mechanism of inheritance is not entirely understood, but it is widely accepted to follow a maternal lineage with only rare instances of paternal mtDNA being present after fertilization.

The total number of mitochondrial genomes varies within different cell types, as well as within the mitochondria of one cell. Through a video-intensified photon counting microscope system, it was determined in human ovarian carcinoma cells that mitochondria contain a mtDNA copy number between 1 and 15 with most of the mitochondria containing between 2 and 6 copies (70). The total number of genomes per cell of course depends upon the number of mitochondria in the cell, which is largely dependent on the energy needs of the tissue type. For instance, leukocytes average 350 mtDNA copies per cell (49); where as myocardial cells average more than 6,000 mtDNA copies per cell (54). The mitochondrial genome also exhibits heteroplasmy, which is the presence of more than one type of mtDNA genome within a cell or individual.

Heteroplasmy contributes heavily to certain genetic diseases, where the mutation burden of mtDNA determines the presence of the disease and occasionally the severity of the condition. The amount of mutated mtDNA must reach a certain threshold for certain diseases to occur. Copy number and heteroplasmy have also been implicated in age related illnesses, as both properties change in a tissue specific manner throughout an individual's life span (91). The constant exposure to reactive oxygen species in the mitochondria makes the mtDNA particularly susceptible to mutations. Given the mitochondria's diverse functional abilities and complex genetic control, it is easy to see how slight deviations within mitochondria could lead to devastating diseases.

B. Mitochondrial Diseases and Dysfunctions

1. Age Related Diseases

Mitochondrial diseases have a wide spectrum of clinical presentations, as well as a variety of inheritance patterns such as maternal, Mendelian, or a combination of both. This can make generating a diagnosis rather difficult, as the same phenotype could be caused by a different mutation, and the same mutation could lead to a completely different condition depending on the quantity of the mutated mtDNA, or the cell type in which the mutation resides (73, 92). Despite this drastic variability, mitochondrial diseases generally affect tissues with high-energy requirements such the central nervous system, liver, kidneys, endocrine system, and skeletal and cardiac muscles (19). Dysfunctions within mitochondria most notably contribute to age related diseases, neurodegenerative diseases, and early and late onset genetic disorders.

The process of aging is still somewhat a mystery, but problems in mitochondria have long been implicated as a possible causal agent. Aging results in a functional decline in various organ systems that coincide with a functional decline in the mitochondrial respiratory chain. It is also known that mtDNA mutations increase in aging animals and humans leading to mitochondrial dysfunction. An increase in reactive oxygen species (ROS) production is also observed (79). This has led to what is known as the Mitochondrial Free Radical Theory of Ageing (MFRTA). This theory attributes an increase in ROS to an increase in mtDNA damage, which leads to mitochondrial dysfunction and further ROS production ultimately resulting in aging (34). This theory is based on animal studies that suggest lower ROS levels result in longer lifespans. There are however some detractors from the MFRTA that suggest an increase in mtDNA mutations is the actual cause of aging, and the ROS increase is only supplementary. As evidence, studies have not shown a correlation between antioxidant defenses and life span (8). Further studies are

needed to elucidate the exact mechanisms of aging, but ROS and mtDNA mutation accumulation both seem to contribute. MtDNA mutations also play a role in several neurodegenerative diseases.

2. Neurodegenerative Diseases

Spinal Muscular Atrophy (SMA) is a neuromuscular disorder characterized by skeletal muscle weakness and atrophy as a result of losing lower motor neurons in the spinal cord. Most cases are caused by a mutation in the survival motor neuron gene (SMN1). The quantity of mtDNA and respiratory chain enzyme activities are significantly reduced in the patient's muscle tissues, which researchers regard as secondary to the original muscle wasting. However, there have been patients exhibiting the various pathologies associated with SMA while lacking a mutation in SMN1. These patients have depleted levels of mtDNA or mutations in the cytochrome c oxidase assembly gene resulting in their clinical phenotype (36). The entirety of this mechanism is not understood.

Parkinson's disease (PD) is the second most common neurodegenerative disorder. Evidence is mounting that mitochondrial dysfunction leads to the nigrostriatal neuronal cell death seen in both neurotoxin-induced and genetic mutant-associated forms of PD. Neurotoxins such as paraquat, rotenone, and 1-methyl-4-phenyl-1, 2, 3, 6-tetrahydropyridine (MPTP) directly inhibit mitochondrial complex I activities resulting in PD phenotypes. The neurotoxins also interfere with mitochondrial dynamic regulations leading to fragmented mitochondria due to increased fission reactions. The genetic form of PD sees mutations in nuclear genes that associate with vital mitochondrial functions such as mitophagy, mitochondrial dynamics, redox signaling, and mitochondrial protein import. As a result, ROS production is increased. Further evidence for mitochondrial dysfunction as a contributing factor to PD is seen when PD

phenotypes are reduced in animal models as a result of therapeutics targeted to inhibit mitochondrial dysfunction (50). Mitochondria are being investigated as a possible area of treatment for PD.

Alzheimer's Disease (AD) is the most common neurodegenerative disorder, and it is characterized by a loss of cholinergic neurons leading to memory loss and behavioral impairments. Amyloid precursor protein and amyloid-β, which are found in mitochondrial membranes and associate with mitochondrial proteins, are elevated in AD and contribute to mitochondrial dysfunction. AD patients have mitochondria that produce excess ROS, have increased permeability, and reduced membrane potential. Excess amyloid precursor protein and amyloid-β may also affect mitochondrial dynamic fusion/fission, mitophagy, and disrupt the ETC (57). Potential therapeutics will likely need to address the mitochondrial dysfunction seen in AD patients.

3. Early and Late Onset Genetic Diseases

Mitochondrial diseases as a whole have a prevalence of 1 in 5000 live births (72). Diseases may occur as a result of inherited mutations in nDNA or mtDNA, which has a 3-fold higher mutation rate respectively (86). Due to the multi-functional nature of mitochondria, mutations leading to dysfunction can result in abnormal calcium signaling, excessive ROS production, dysregulation of apoptosis, and of course energy deficiencies (97). Many conditions are multisystemic in nature, but some diseases are specific to one tissue type such as Leber's hereditary optic neuropathy (LHON) (74). LHON leads to acute loss of central vision, and is most commonly the result of one of three possible homoplasmic point mutations in mtDNA genes that code for subunits in complex I (69). Most conditions, however, are caused by heteroplasmic mutations, where only some copies of the mtDNA have the mutation.

This is the case with MELAS (mitochondrial encephalomyopathy with lactic acidosis and stroke like episodes). 80% of MELAS cases are caused by the point mutation m.3243A>G, which affects mt-tRNA$^{Leu(UUR)}$. The mutation results in a decreased rate of protein synthesis leading to energy deficiencies in addition to the symptoms included in the name of the disease. Although this mutation is shown to cause MELAS, relatively few patients with this mutation develop MELAS. Instead, maternally inherited diabetes and deafness (MIDD) is more commonly seen, as well as a mixture of symptoms from both MELAS and MIDD (55). This highlights the complexity of mitochondrial diseases, as they are dependent on numerous factors and often exhibit clinical heterogeneity.

Leigh's disease (also known as subacute, necrotizing encephalopathy) is a mitochondrial condition that exhibits the largest genetic heterogeneity, and also shows great phenotypic variability. Leigh's disease is characterized by focal, bilateral lesions in the basal ganglia, thalamus, brainstem, and other areas of the brain. Other symptoms associated with Leigh's disease are muscle hypotonia, dystonia, seizures, ataxia, nystagmus, breathing irregularities, cardiomyopathy, gastrointestinal distress, and many others (2, 22). Mutations in nuclear or mitochondrial genes that code for subunits of the respiratory chain are the cause of Leigh's disease.

This research project focuses on the mutation m.8993 T>G. The mutation is present in the ATP6 gene of mitochondria, which codes for a subunit of the F_o component of ATP synthase. The m.8993 T>G mutation results in a substitution of arginine for leucine (85). It was originally believed that this mutation altered effective proton transfer, as it affects the pore-forming unit of ATP synthase (28). Other research suggests that the mutation affects the c ring subunits ability to rotate (77). With a mutation load above 95%, this mutation leads to Leigh's disease typically

before the age of two. This same mutation at lower loads leads to an adult onset disorder known as NARP (neurogenic muscle weakness, ataxia, and retinitis pigmentosa). The severity of the condition is often dependent on the percentage of mutated mtDNA (38). Because the m.8993 T>G form of Leigh's disease requires such a high percentage of mutated mtDNA and reduced phenotypes are seen at lower mutation loads, it is conceivable that altering the mutation burden could serve as a possible therapy. Only palliative care is available for Leigh's disease and all of the previously discussed conditions. Mitochondrial dysfunction can lead to a vast amount of complex diseases. Cell based models provide an effective means of studying these diseases, and could possibly allow for patient specific treatments.

C. Cell Based Models

1. Cybrid Model

A lack of an effective model for studying mitochondrial disorders has led to a variety of inventive cell based model strategies in an attempt to mimic disease states. The first generation of these cell based models was the cytoplasmic hybrid (cybrid), which involved fusing mtDNA derived from platelets with mtDNA depleted neuroblastoma cells. Cybrids with mtDNA extracted from patients with AD, PD, and MELAS have been successful in displaying similar disease phenotypes to their respective pathologies including respiratory chain defects, increased oxidative stress, and alterations in calcium homeostasis (7, 24, 15). However, the cybrid model has the limitation that the host cells are tumor cells. These cells would thus be expected to have an altered cell cycle progression and mitochondrial biogenesis. Also, it is not known to what degree platelet derived mtDNA matches the genome of other cell types (90).

A modification of the cybrid model has been used to generate trans-mitochondrial mito-mice. In this model, mutated (13997 G>A) mtDNA from mouse lung carcinoma cells was implanted in mtDNA depleted mouse embryonic stem cells (ESCs). The engineered ESCs were then implanted into pseudopregnant females, and the progeny were characterized as having successfully received the mutant mtDNA. The results displayed the expected complex I defects and lactate overproduction, but to a lesser degree than the mtDNA donor mouse lung carcinoma cells. In addition, other symptoms that were expected such as ROS overproduction, LHON phenotypes, and tumor formation were not observed (98). Although this model used ESCs as the host for the mutated mtDNA as opposed to tumor cells, the results did not fully display the expected disease state due to some compensatory mechanism. A human cell based model would need to be produced for further studies.

2. Neural Progenitor Model

An improvement to the cybrid model for investigating neurodegenerative diseases is the use of human neural progenitor (hNP) cells. Neural progenitor cells can differentiate into neurons, astrocytes, and oligodendrocytes providing possible models for disease states and potential therapeutics for various conditions. Neural progenitors can be morphologically characterized by the formation of radially organized columnar epithelial cells known as “neural rosettes,” and possess a high nuclear-cytoplasmic ratio indicative of actively dividing cells (13, 20). Gene expression or immunocytochemistry assays for markers such as Nestin, Musashi 1, SOX2, and polysialylated neural cell adhesion molecule also confirm cells as neural progenitors (14). Uniform neural progenitor populations can be created from hESCs when supplemented with select medium components. The development of these procedures was critical in being able

to generate an unlimited lineage-restricted cell source that can maintain a stable chromosome number for an effective cell based model (14, 78, 32).

This new technology was used in the development of a model to study the genetic mitochondrial disease known as Leber's hereditary optic neuropathy (LHON). In this study, neural progenitors were treated with dideoxycytidine (ddC), which reduces the endogenous mtDNA. There was no loss in hNP phenotypic markers after this procedure. The cells were then transfected with recombinant human mitochondrial transcription factor A complexed with mtDNA that harbored the pathogenic mtDNA G11778A mutation known to be a causal agent for LHON. The expression of the pathogenic RNA was confirmed, and the hNPs maintained their ability to differentiate after the transfection (31). Although successful in recreating this disease state, the challenges of this process are in ddC treating the hNPs while maintaining their hNP marker expression, and adequately transfecting the desired mutant DNA. This process may be difficult to replicate with more complex conditions, and thus alternatives were investigated.

3. Induced Pluripotent Stem Cell Model

Reprogramming technologies allow researchers to create induced pluripotent stem cells (iPSCs) from adult cell types. These cells types exhibit prolonged self-renewal and the ability to differentiate into multiple cell lineages. Thus, iPSCs could serve as a cell-based model for drug screening, understanding disease mechanisms, and engineering patient specific cell lines for possible therapies (87). Reprogramming was first carried out via retroviral-mediated transfection of transcription factors known to be necessary for pluripotency (82, 83). Although successful in generating iPSCs for basic research, there was concern about using this technology for therapeutic applications, as the viral factors integrate with the genome causing the potential for cancers to develop. Excisable transposon and non-integrative plasmid strategies were

subsequently developed. These methods resolve the problem of genome integration, but are labor intensive and produce low yields of iPSCs (93, 68, 51). An improvement to these strategies is the use of modified mRNAs encoding the reprogramming factors OCT4, SOX2, c-MYC, KLF4, and LIN28A (93). In addition to taking fewer days and generating higher yields, mRNA reprogramming allows for dosage control of multiple proteins simultaneously, thus permitting much more control of the reprogramming process (51). It is also reasonable to conclude that upon further investigation, direct differentiation procedures can be developed using appropriate mRNAs (93).

Reprogramming somatic cells from diseased patients to iPSCs has been used to generate effective cell-based models for neurodegenerative disorders such as SMA, PD, and Amyotrophic Lateral Sclerosis (99, 1, 16, 11). Recently this method has been applied to the study of cell-type specific disease phenotypes in the mitochondrial disease MELAS. As previously stated, it is known that the most common cause of MELAS is a mutation in the mtDNA. Reprograming has allowed for the study of how the mutation results in varying severities of clinical symptoms (29). In order for iPSCs to be used as an effective cell based model, it must be verified that reprogramming has not caused significant alterations to the genome. It has been shown that retroviral reprogramming led to mtDNA mutations that were not present in parental cells (63). This is a very important aspect to monitor before conclusions can be made in future studies.

D. Summary

The successful development of reprogramming technologies has enabled researchers to investigate diseases in a patient and cell specific manner. This method can be particularly useful in studying conditions that display clinical variability among patients, as well as conditions that affect certain cell types differently. As both conditions hold true in Leigh's disease 8993 T>G, it

is our hope to develop an iPSC model that accurately reflects the disease characteristics seen in the patient from which the original cells were derived.

Early reprogramming methods led to mutations that were not seen in the parent cell. Because mRNA reprogramming methods are still relatively new, it is not known if this process alters the genome of the reprogrammed cells. Before more investigative disease studies can be conducted with our Leigh's 8993 T>G reprogrammed cell line, it must first be confirmed that the iPSCs maintain this mutation. Based on the background information, we propose to investigate the following specific aims.

Specific Aim (I) **Detect the presence of the 8993 T>G mtDNA mutation in iPSCs of various passage numbers and differentiated derivatives.**

This preliminary data is essential to ensure that the disease-causing agent is still present in the reprogrammed cells and differentiated cell types.

Specific Aim (II) **Quantify the mutation burden in patient derived fibroblasts, iPSCs of various passage numbers, and differentiated derivatives.**

This data will display the exact percentage of the 8993T>G mutation that is present in the mtDNA of the original patient derived fibroblasts, iPSCs, and differentiated derivatives. Experiments under this specific aim focus on investigating if the mutation burden is maintained through reprogramming, several passages, and differentiation into various cell types. The results of these experiments could provide support for this method as a viable option of developing patient specific cell based models to investigate Leigh's disease 8993 T>G.

CHAPTER 2: MATERIALS AND METHODS

A. MtDNA Isolation

Before the mtDNA can be sequenced, it must be isolated from whole cell pellets, purified, and quantified.

Control Cell Lines	Experimental Cell Lines
Human Foreskin Fibroblast passage 13 (BJ fib p13)	Leigh's Patient Fibroblast passage 7 (FB1 fib p7)
Induced Pluripotent Stem Cell passage 21 (BJ iPSC p21)	Leigh's Induced Pluripotent Stem Cell passage 9 (FB1 iPSC p9)
	Leigh's Induced Pluripotent Stem Cell passage 15 (FB1 iPSC p15)
	Leigh's Induced Pluripotent Stem Cell passage 21 (FB1 iPSC p21)
Induced Pluripotent Stem Cell that has been spontaneously differentiated passage 24 (BJ Diff p24)	Leigh's Induced Pluripotent Stem Cell that has been spontaneously differentiated passage 24 (FB1 Diff p24)

Table 1: List of cell samples used in all experiments.

The FB1 samples were derived from a Leigh's patient donor, and are expected to have the 8993 T>G mutation. All of the BJ samples are expected to have the wild type 8993 T, thus, serving as the control. All samples will undergo the same processing.

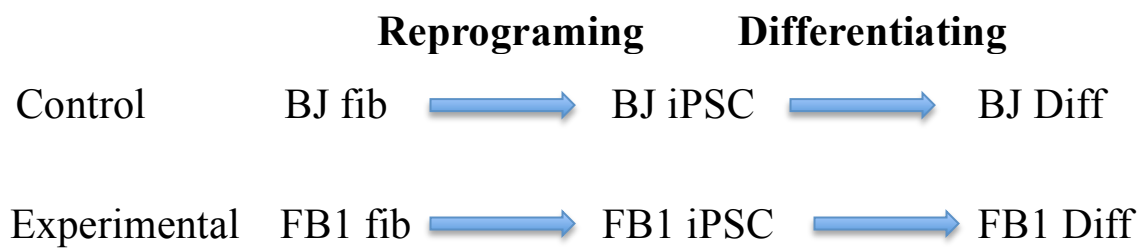

Figure 1: Schematic of sample derivation prior to our experiments.

The mRNA based reprogramming procedure was carried out according to established protocols (62), resulting in the generation of iPSCs. Spontaneous differentiation was carried out by embryoid body formation according to established protocols (37). This form of differentiation results in cell types from all three germ layers. These procedures were carried out prior to our experiments.

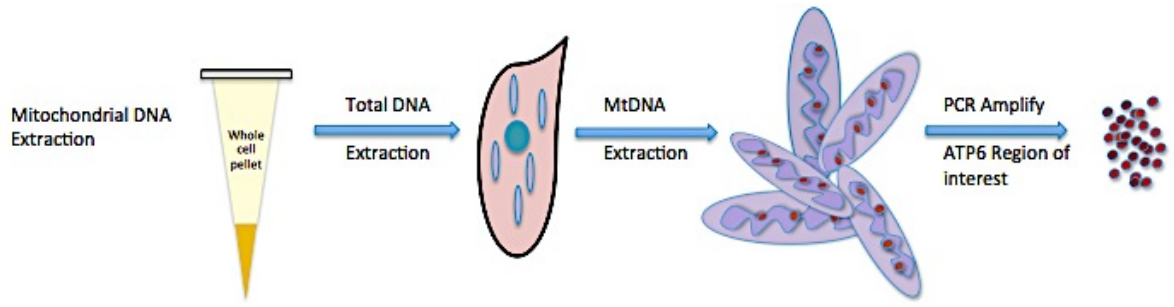

Figure 2: Schematic of mtDNA extraction.

First, total DNA was extracted from whole cell pellet. MtDNA was then extracted by enzymatically degrading all non-circular forms of DNA. Finally, the region of interest within the ATP6 gene was PCR amplified.

1. Extracting MtDNA From Whole Cell Pellets

Cell pellets containing approximately 500,000 cells were removed from the freezer to thaw. The QIAamp DNA mini kit manufacturer protocol was followed to extract total DNA, and the details can be seen in Appendix i (Qiagen, Valencia, CA, USA). This results in an elution of 80 µL of distilled water (dH_2O) and total DNA from all cells. In order to obtain the circular mtDNA, all other DNA was degraded using the Plasmid-Safe ATP-Dependent DNase (Epicentre, Madison, WI, USA). This product selectively degrades all non-circular DNA molecules. The manufacturer recommended mini-preparation protocol was followed, details of which can be found in Appendix i. The 50 µL solutions containing the mtDNA were further treated with 1 µL of RNaseA for 1 hour at 37°C to further avoid any non-mtDNA nucleic acids. It is expected that at this point, the mtDNA should be intact, and all other forms of DNA should be degraded. The samples were further processed prior to use in sequencing protocols.

2. Further Purification and Gel Extraction

In order to rid the mtDNA samples of previously used enzymes, salts, etc., the samples were cleaned using the UltraClean 15 DNA Purification Kit (Mo Bio, Carlsbad, CA, USA), details of the protocol can be found in Appendix ii. To ensure the mtDNA was maintained in a 16kb circle, the samples were run on a 0.8% agarose gel, and the 16kb band that appeared for each sample was extracted from the gel. The methods for creating and running the gel, as well as the results can be found in Appendix ii. Because the samples were extracted from an agarose gel, they needed to be cleaned again using the UltraClean 15 DNA Purification Kit with a slightly modified protocol to get rid of the agarose, details of which are present in Appendix ii. With the mtDNA isolated and purified, the samples were prepared for sequencing.

B. Sample Preparation for Sequencing

The previous procedures resulted in a 30 µL solution of dH_2O with an unknown quantity of mtDNA. The amount of mtDNA needed to be quantified and diluted to meet the specifications for Sanger sequencing and whole exome next-gen sequencing.

1. Quantification and Dilution

The mtDNA was quantified using a NanoDrop One UV/Vis Spectrophotometer (Thermo scientific, Wilmington, DE, USA). A blank of 1.5 µL of dH_2O was used to establish a zero, and 1.5 µL of each sample was used to find the concentration. Concentration results can be found in Appendix iii. Exome sequencing requires approximately 25 ng of DNA, and the samples were diluted accordingly. Sanger sequencing, however, requires the area of interest (Region of ATP6 gene containing 8993) to be PCR amplified, purified, and diluted to a concentration of 10ng/µL.

2. PCR and Preparations for Sanger Sequencing

Primers were generated using the human mtDNA sequence provided by mitomap.org, and IDT's PrimerQuest tool (IDT, Coralville, Iowa).

Gene	Direction	Sequence	GC%	Product Length
ATP 6	Forward	TATCGAAACCATCAGCCTACTC	45.5	100 bp
	Reverse	GCTTCCAATTAGGTGCATGAG	47.6	

Table 2. Primer information for region of ATP 6

The 100 bp amplified sequence contains the 8993 site.

A standard PCR was carried out using the Takara Taq PCR Amplification Kit (Clontech, Mountain View, CA, USA). A detailed protocol of the reaction mixture and the cycle information can be seen in Appendix iv. 10 µL of the PCR product for each sample was run on a 2% agarose gel to confirm proper amplification of the region of interest. The methods for creating and running the gel, as well as the results can be found in Appendix ii. After gel confirmation, the PCR products were cleaned again using the UltraClean 15 DNA Purification Kit (Mo Bio, Carlsbad, CA, USA). The cleaned PCR products were quantified using a NanoDrop One UV/Vis Spectrophotometer (Thermo scientific, Wilmington, DE, USA), and diluted to 10 ng/µL with dH_2O for Sanger sequencing. Also, the primers were diluted to 20ng/µL for Sanger sequencing. The results from the NanoDrop analysis are presented in Appendix iii.

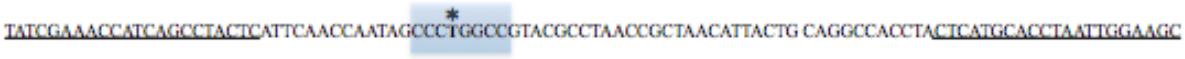

Figure 3: Sequence of amplified product.

The 8993 position is denoted with an asterisk. We are expecting all of the BJ derived samples to have a T at this site, and all of the FB1 samples to have a G at this site.

C. Sanger Sequencing, Next-gen Sequencing for Whole Exome, and Accompanying Sequence Analysis

All sequencing was carried out in collaboration with the Virginia Commonwealth University Nucleic Acids Research Facility.

1. Sanger Sequencing and Analysis

Sequencing reactions were carried out with the forward and reverse primers. The cycle sequencing reaction was carried out on a 96-capillary 3730XL (Applied Biosystems, Foster City, CA, USA) with BigDye Taq FS Terminator V 3.1. The genotyping and fragment sizing was done on a 3130XL (Applied Biosystems, Foster City, CA, USA). Details of the cycle sequencing reaction and the precipitation protocol can be seen in Appendix v. The files generated from the sequencing were observed using CodonCode Aligner (CodonCode Corporation, Centerville, MA, USA).

2. Next-gen Sequencing of Whole Exome and Analysis

The DNA concentration was verified using a Qubit fluorometer (Thermo scientific, Wilmington, DE, USA). Instead of the standard DNA fragmentation, an enzymatic fragmentation was performed using the KAPA Frag Enzyme from the KAPA HyperPlus Library Preparation Kit (KAPA Biosystems, Wilmington, MA, USA). This alternative was performed in order to increase yield during the fragmentation step. Fragmented DNA was purified using Ampure beads (Beckman Coulter, Brea, CA, USA). DNA libraries were prepared using the Accel-NGS 2S Plus DNA Library Kit (Swift Biosciences, Ann Arbor, MI, USA). 10 PCR cycles were carried out during the Library Amplification step. The final libraries were analyzed with a 2100 Bioanalyzer to assess library size distribution (Agilent Technologies, Santa Clara, CA).

DNA libraries were quantified with the KAPA Library Quantification Kit to ensure accuracy (KAPA Biosystems, Wilmington, MA, USA). Based on the qPCR results, the DNA libraries were compiled in equimolar amounts and sequenced with the HiSeq 2500 using TruSeq v3 reagents according to the 2 x 100 bp protocol (Illumina, San Diego, CA, USA).

The file generated from sequencing was separated out into FASTQ files using bcl2fastq software version 2.17 (Illumina, San Diego, CA, USA). These files were aligned to the mtDNA reference human genome 19 with Burrows-Wheeler Alignment Tool (45). The alignment tool generates Sequence Alignment Map (SAM) files, which are sorted based on the coordinates of the sequence. The SAM files are then converted to a compressed form, BAM format, using SAMTools. PCR duplicates were removed from the alignment using the Picard toolkit (Broad Institutes, Cambridge, MA, USA). Finally, the BAM format files were sent to Atlas2 to generate variant calling files (VCFs) (Human Genome Sequencing Center, Houston, TX, USA). Integrative Genomics Viewer (IGV) was used to view the sequences (88), while the VCFs were viewed with a word processor. The filter settings on the VCFs can be seen in Appendix vi.

CHAPTER 3: RESULTS

A. Sanger Sequencing Results

It was expected that the 8993 T>G mutation would be present in the original fibroblast taken from the Leigh's disease patient, as well as in the iPSCs of various passage numbers and differentiated cells derived from the patient fibroblast. In order to confirm the presence of the mutation, the mtDNA was extracted from whole cell pellets, and our region of interest within the ATP6 gene was PCR amplified. The PCR product was purified and quantified to the appropriate specification. This allowed for Sanger sequencing of the specific ATP6 region containing the 8993 site. All procedures were conducted as outlined in the materials and methods section. Sanger sequencing of our samples was necessary to confirm the presence of the disease causing mutation after reprogramming and spontaneous differentiation. The results demonstrate that the 8993 T>G mutation is present in all FB1 samples (FB1 fib p7, FB1 iPSC p9, FB1 iPSC p15, FB1 iPSC p21, and FB1 Diff p24). (Figure 4-6). Verifying the presence of the mutation was a necessary step prior to the quantification of mutation burden using Next-gen sequencing for whole exome.

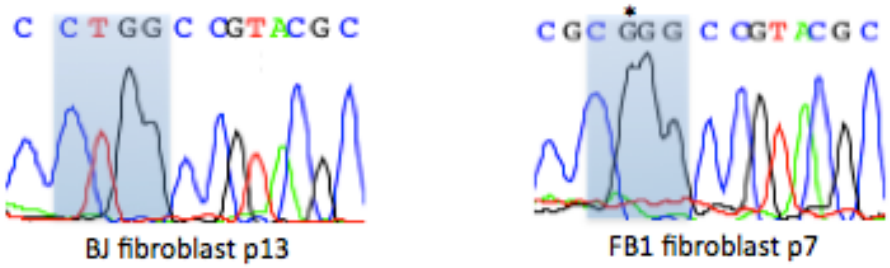

Figure 4: Sanger sequencing results of FB1 fibroblast (BJ fibroblast control).

PCR amplified products were Sanger sequenced, and the sequencing results were viewed using CodonCode Aligner. The mutation is seen in the FB1 fibroblast sample, and not in the BJ fibroblast sample. The asterisk mark the point mutation**.**

Back To Table of Contents

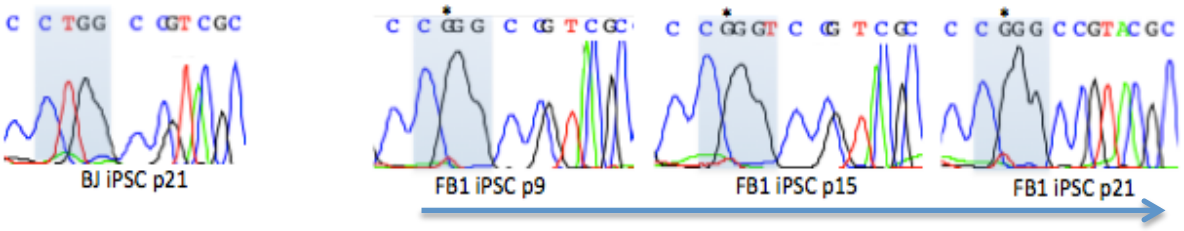

Figure 5: Sanger sequencing of FB1 iPSC across multiple passages (BJ iPSC control).

PCR amplified products were Sanger sequenced, and the sequencing results were viewed using CodonCode Aligner. The mutation is seen in all FB1 iPSC samples, and not in the BJ iPSC sample. The asterisks mark the point mutations**.**

Back To Table of Contents

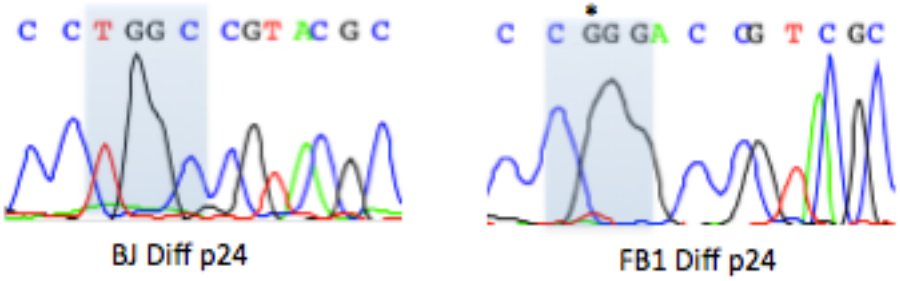

Figure 6: Sanger sequencing of FB1 differentiated (BJ Diff control).

PCR amplified products were Sanger sequenced, and the sequencing results were viewed using CodonCode Aligner. The mutation is seen in the FB1 differentiated sample, and not in the BJ differentiated sample. The asterisk marks the point mutation**.**

Back To Table of Contents

B. Next-gen Sequencing for Whole Exome Results

With the presence of the mutation confirmed, the percentage of mutation burden in each sample was measured using high-throughput Next-gen sequencing for whole exome. This strategy has previously been utilized to effectively measure heteroplasmies in the mitochondrial genome (10, 84, 47). The mtDNA was extracted from whole cell pellets, and then purified before sequencing. The sequencing results yielded a range of total sequence reads between 388 and 2031 at the 8993 position in the different cell samples. This large of a sample size allows us to be confident about the percentages measured. As expected, BJ fib, BJ iPSC, and BJ Diff possessed mostly the wild type thymine with only a few sequences containing the mutated guanine. The Leigh's patient sample FB1 fibroblast exhibited the mutation in 85 % of the sequences read. The iPSCs of various passage numbers and the differentiated cell sample displayed similar mutation levels with a range of 80-88% (Figure 7 and Table 3).

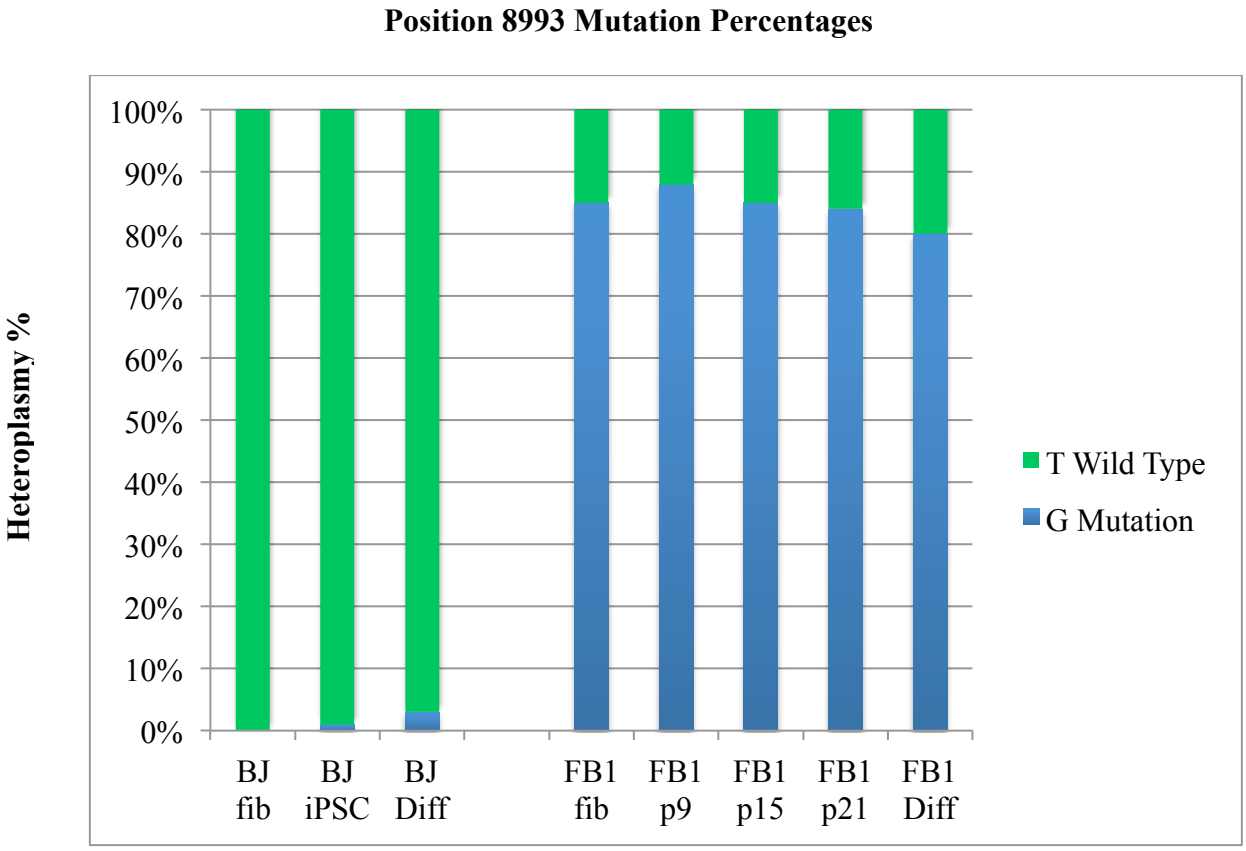

Figure 7: Heteroplasmy data for all samples at position 8993.

The extracted mtDNA was Next-gen sequenced for whole exome. The sequencing results were compiled, and the results were analyzed with the Integrative Genomics Viewer. This allows us to view heteroplasmic sequences with an exact measure of the variants. The BJ samples exhibited very low amounts of the T>G mutation at the 8993 position, and the FB1 samples exhibited a 8993 T>G mutation burden in the range of 80-88%. The variant calling files filter settings can be seen in Appendix vi.

Sample Name	Total Number Sequenced	8993 T	8993 G	Percentage of Mutation
BJ fibroblast	689	689	0	0
BJ iPSC	1812	1801	11	1
BJ Differentiated	388	377	9	3
FB1 fibroblast	548	84	464	85
FB1 iPSC p9	1987	234	1753	88
FB1 iPSC p15	2031	305	1726	85
FB1 iPSC p21	589	92	497	84
FB1 iPSC Differentiated	1000	203	797	80

Table 3: Heteroplasmy data for all samples at position 8993.

The extracted mtDNA was Next-gen sequenced for whole exome. The sequencing results were compiled, and the results were analyzed with the IGV. This allows us to view heteroplasmic sequences with an exact measure of the variants. The total number of reads per sample at the 8993 position ranged between 388 and 2,031. This is more than enough reads to make accurate determinations for sample 8993 T>G mutation burden. The BJ samples displayed a mutation burden between 0-3%, and the FB1 samples displayed a mutation burden between 80-88%. The variant calling files filter settings can be seen in Appendix vi.

CHAPTER 4: DISCUSSION AND FUTURE DIRECTIONS

Despite the mitochondrial genome being rather small, effectively researching the pathogenesis of mitochondrial diseases caused by mtDNA mutations has been difficult. Leigh's disease has the added complexity of being dependent upon reaching a threshold of mutation burden in a tissue specific manner. Our methods included the use of Sanger sequencing, Next-gen sequencing, and subsequent analysis of the results to confirm the presence of the 8993 T>G mutation in all Leigh's patient derived cell samples. The mutation was detected in all FB1 samples, and the mutation burden was maintained at a consistently elevated percentage through reprogramming, several passages, and spontaneous differentiation. Thus, our experiments have resulted in the creation of an iPSC line with a comparable mutation burden to that of the Leigh's patient fibroblast from which it was derived. Generating this cell line with the disease-causing mutation intact is a very important step in confirming reprogramming technologies as a viable option of creating a cell based model for Leigh's disease.

Clinically, Leigh's disease displays variability among patients and variability among different tissues within individual patients, which can complicate research. Our cell based model addresses both of these issues. An iPSC model can be created specific to a patient. The stem cells could then be directly differentiated into specific cell types of interest such as neurons or myocytes. Further experiments can be carried out to determine how the disease affects specific tissues on a molecular basis. This is a promising approach for the investigation of patient and

Back To Table of Contents

tissue specific pathophysiology, and for generating possible therapeutics for individual patients affected by Leigh's disease and other mitochondrial diseases. The methods used in this study to successfully create this disease model could also be slightly altered in order to investigate other mitochondrial diseases.

In addition to confirming the consistent mutation burden of 8993 T>G, the Next-gen sequencing results also identified a number of other heteroplasmic variants (Table 4). Due to the highly polymorphic nature of the mitochondrial genome, a number of these variants are characterized as normal sequence variants that are not likely to contribute to Leigh's disease. Some of the variants displayed in the FB1 patient samples were also present in the BJ control samples in similar quantites (Table 5). Thus, it is unlikely that these sequence variants contribute to Leigh's disease. Two other variants in the FB1 patient samples were also present in the BJ control samples, but in lower quantities (Table 6). When cross examined with the MitoMap reference, both of these sites were determined to be normal polymorphisms. Also, a number of sequence variants were associated with previously defined mitochondrial haplogroups. It is widely known that haplogroup designations are used in population genetics to denote people with a common ancestory. The haplogroups connected to the FB1 cell line are indicative of European ancestory, which correlates with the origin of the cell line used in this study (Table 7). It would be interesting to see if other patients with Leigh's disease could be connected to similer haplogroups. This information could be beneficial in identifying at risk populations for Leigh's disease.

With the normal variants identified, there were a few remaining sites of interest for possible future studies (Table 8). The 310 T>C mutation is in the hypervariable II region of the mitochondrial genome. This control region of the genome is heavily concentrated with

polymorphisms that have inconclusive affects, but the 310 T>C mutation has been implicated in malignant melanoma, colorectal cancer, and breast cancer (17, 25, 89). The presence of this mutation is detected in these types of cancer patients at a statistically higher amount when compared to control populations. This mutation is expected to hinder replication or transcription of the mitochondrial genome, which could elevate ROS production (89). It is unclear how this mutation might affect Leigh's disease.

Another possible variant of interest is 12358 A>G, which is in the ND5 gene coding for subunit five of NADH dehydrogenase. This mutation is present in a statistically significant higher number of sporadic Creutzfeldt-Jakob disease cases compared to controls. The mutation is reported to be correlated with altered brain pH values. It is hypothesized that this could be caused by a lack of coupling in complex I of the electron transport chain. This variant has not previously been implicated in Leigh's disease.

Our research was focused on the 8993 T>G mutation in the ATP6 gene, however, many Leigh's disease cases are caused by mutations in genes that code for subunits of complex I. Next-gen sequencing of the FB1 Leigh's patient cell line revealed ten sequence variants in genes that code for subunits of complex I. None of these variants have previously been mentioned as causes of Leigh's disease, but it is not inconceivable that they could in some way contribute to the disease state. Cross referencing these variants with other Leigh's patient sequencing results could allow for the determination of their importance to Leigh's disease.

Our results have opened up a few avenues for future areas of research. Because Leigh's disease has more drastic affects on neural cells and myocytes, a possible area of research would be to directly differentiate our iPSC line into these cell types. Specific transcription factors have been used to direct differentiation into neural cell types (40). Direct differentiation to

cardiomyocytes has been difficult in humans, but mouse embryonic fibroblasts have been directed into cardiomyocytes (18). Differentiation strategies are constantly improving. Sequencing studies could be performed again to ensure the 8993 T>G mutation is still intact.

In addition to sequencing for heteroplasmies, another interesting area of research could be connecting the level of mutation burden to the degree of mitochondria dysfunction. Select biomarkers for mitochondrial dysfunction such as carnitine, pyruvic acid, and lactic acid have been used in the past to assess mitochondrial respiration. However, a technology has been developed that allows mitochondrial respiration and glycolysis to be measured simultaneously in live cells. The Seahorse XF(e)24 Extracellular Flux Analyzer can measure the oxygen consumption rate and lactic acid production rate, which are very accurate measures of mitochondrial function. It would be interesting to see if the level of mutation burden quantitatively altered these measurements (44).

Heteroplasmic Variant Site	Locus	FB1 fib %	FB1 p9 %	FB1 p15 %	FB1 p21 %	FB1 Diff %	MitoMap Reference
72 G>A	HVII	86	100	100	99	97	T
149 T>C	HVII	90	100	100	100	100	T
*310 T>C	HVII	20	18	28	25	18	T
1720 G>A	RNR2	87	97	98	99	96	C
2707 G>A	RNR2	88	100	100	100	96	A
4793 A>G	ND2	83	97	99	100	85	A
*5231 G>A	ND2	20	0	0	0	1	G
*5417 G>A	ND2	21	0	0	1	0	G
7028 T>C	COX1	67	99	99	100	94	C
*10325 G>A	ND3	1	0	0	0	18	G
11719 A>G	ND4	82	100	98	100	99	G
*11914 G>A	ND4	28	0	0	0	0	G
*12358 A>G	ND5	18	0	1	0	1	A
*12372 G>A	ND5	21	0	1	0	0	G
12705 T>C	ND5	87	99	99	99	98	C
12879 T>C	ND5	10	0	0	1	0	T
14766 T>C	CYTB	81	100	100	99	86	C
15067 T>C	CYTB	11	0	0	0	0	T
16172 C>T	HVI	89	100	99	100	100	T
16184 C>A	HVI	83	84	98	99	80	C
16257 C>T	HVI	86	99	99	100	97	C
16295 C>T	HVI	88	99	98	100	95	C

Table 4: Other sites of heteroplasmic variants in Leigh's patient cell line.

The extracted mtDNA was Next-gen sequenced for whole exome. The sequencing results were compiled, and the results were analyzed with the Integrative Genomics Viewer. This allows us to view heteroplasmic sequences with an exact measure of the variants. In addition to the 8993 site, the sequencing results yielded a number of other variants when compared to the human genome 19 reference. Yellow highlighted variant sites indicate that the control samples contained this variant with similar percentages. Green highlighted variant sites indicate that the control samples contained this variant, however, the percentages of the variant in the control samples were much

lower than the percentages in the FB1 samples. The MitoMap nucleotide was included to provided a secondary reference sequence. The variant calling files filter settings can be seen in Appendix vi.

Heteroplasmic Variant Site	Locus	FB1 fib %	FB1 p9 %	FB1 p15 %	FB1 p21 %	FB1 Diff %	BJ fib %	BJ iPSC %	BJ Diff %	MitoMap Reference
149 T>C	HVII	90	100	100	100	100	99	100	100	T
12705 T>C	ND5	87	99	99	99	98	99	100	100	C
16172 C>T	HVI	89	100	99	100	100	100	100	100	T
16184 C>A	HVI	83	84	98	99	80	97	88	91	C

Table 5: Heteroplasmic variants in Leigh's patient cell line similar in BJ control.

The extracted mtDNA was Next-gen sequenced for whole exome. The sequencing results were compiled, and the results were analyzed with the Integrative Genomics Viewer. These four sites are the same yellow highlighted sites from Table 4. Because the BJ control samples contain these variants at similar quantities, it is likely that these are natural variants that do not contribute to Leigh's disease. Cross referencing the variants with the MitoMap reference revealed that the 12705 and 16172 sequences are considered normal polymorphisms. The variant calling files filter settings can be seen in Appendix vi.

Heteroplasmic Variant Site	Locus	FB1 fib %	FB1 p9 %	FB1 p15 %	FB1 p21 %	FB1 Diff %	BJ Fib %	BJ iPSC %	BJ Diff %	MitoMap Reference
2707 G>A	RNR2	88	100	100	100	96	0	1	27	A
14766 T>C	CYTB	81	100	100	99	86	2	0	18	C

Table 6: Heteroplasmic variants in Leigh's patient cell line different in BJ control.

The extracted mtDNA was Next-gen sequenced for whole exome. The sequencing results were compiled, and the results were analyzed with the Integrative Genomics Viewer. These sites are the same green highlighted sites from Table 4. Cross referencing the variants with the MitoMap reference revealed that both 2707 and 14766 are considered normal polymorphisms. The variant calling files filter settings can be seen in Appendix vi.

Sequence Variant	Associated Haplogroup(s)
4793	H7
7028	Pre-HV, HV, N, R, U
11719	N, R, U, HV
12372	U
12705	N
12879	U1
14766	Pre-HV, N, R, U
16172	U6
16257	T3

Table 7: Leigh's patient sequence variant and associated haplogroup.

The extracted mtDNA was Next-gen sequenced for whole exome. The sequencing results were compiled, and the results were analyzed with the Integrative Genomics Viewer. A number of the detected variants are associated with defined haplogroups. These haplogroups are associated with people of European descent, which makes sense as the Leigh's patient donor is from Europe. It is unclear as to whether these specific haplogroups are connected to Leigh's disease.

Heteroplasmic Variant Site	Locus	FB1 fib %	FB1 p9 %	FB1 p15 %	FB1 p21 %	FB1 Diff %	MitoMap Reference
310 T>C	HVII	20	18	28	25	18	T
5231 G>A	ND2	20	0	0	0	1	G
5417 G>A	ND2	21	0	0	1	0	G
10325 G>A	ND3	1	0	0	0	18	G
11914 G>A	ND4	28	0	0	0	0	G
12358 A>G	ND5	18	0	1	0	1	A
12372 G>A	ND5	21	0	1	0	0	G

Table 8: Heteroplasmic variants possibly implicated in Leigh's disease.

The extracted mtDNA was subjected to whole exome next-gen sequencing. The sequencing results were compiled, and the results were analyzed with the Integrative Genomics Viewer. This table includes variants that were not ruled out by virtue of being consistent with the BJ control, MitoMap reference, or a known haplogroup. Sites 310 and 12358 are associated with other diseases, but it is unknown as to whether these variants or the any of the others contribute to Leigh's disease. The variant calling files filter settings can be seen in Appendix vi.

REFERENCES

1. Badger, J.l., O. Cordero-Llana, E.m. Hartfield, and R. Wade-Martins. "Parkinson's Disease in a Dish – Using Stem Cells as a Molecular Tool." *Neuropharmacology* 76 (2014): 88-96.
2. Baertling, F., R. J. Rodenburg, J. Schaper, J. A. Smeitink, W. J. H. Koopman, E. Mayatepek, E. Morava, and F. Distelmaier. "A Guide to Diagnosis and Treatment of Leigh Syndrome." *Journal of Neurology, Neurosurgery & Psychiatry* 85.3 (2013): 257-65.
3. Ballmoos, Christoph Von, Alexander Wiedenmann, and Peter Dimroth. "Essentials for ATP Synthesis by F 1 F 0 ATP Synthases." *Annu. Rev. Biochem. Annual Review of Biochemistry*78.1 (2009): 649-72.
4. Bayrhuber, M., T. Meins, M. Habeck, S. Becker, K. Giller, S. Villinger, C. Vonrhein, C. Griesinger, M. Zweckstetter, and K. Zeth. "Structure of the Human Voltage Dependent Anion Channel." *Proceedings of the National Academy of Sciences* (2008).
5. Benard, Giovanni, and Rodrigue Rossignol. "Ultrastructure of the Mitochondrion and Its Bearing on Function and Bioenergetics." *Antioxidants & Redox Signaling* 10.8 (2008): 1313-342.
6. Beraud, Nathalie, Sophie Pelloux, Yves Usson, Andrey V. Kuznetsov, Xavier Ronot, Yves Tourneur, and Valdur Saks. "Mitochondrial Dynamics in Heart Cells: Very Low Amplitude High Frequency Fluctuations in Adult Cardiomyocytes and Flow Motion in Non Beating Hl-1 Cells." *Journal of Bioenergetics and Biomembranes J Bioenerg Biomembr* 41.2 (2009): 195-214.
7. Borland, M. Kathleen, K.p. Mohanakumar, Jeremy D. Rubinstein, Paula M. Keeney, Jing Xie, Roderick Capaldi, Lisa D. Dunham, Patricia A. Trimmer, and James P. Bennett. "Relationships among Molecular Genetic and Respiratory Properties of Parkinson's Disease Cybrid Cells Show Similarities to Parkinson's Brain Tissues." *Biochimica Et Biophysica Acta (BBA) – Molecular Basis of Disease* 1792.1 (2009): 68-74.
8. Bratic, Ana, and Nils-Göran Larsson. "The Role of Mitochondria in Aging." *Journal of Clinical Investigation J. Clin. Invest.* 123.3 (2013): 951-57.
9. Brini, Marisa, Paolo Pinton, Michael P. King, Mercy Davidson, Eric A. Schon, and Rosario Rizzuto. "A Calcium Signaling Defect in the Pathogenesis of a Mitochondrial DNA Inherited Oxidative Phosphorylation Deficiency." *Nature Medicine* 5.8 (1999): 951-54.
10. Carroll, C. J., V. Brilhante, and A. Suomalainen. "Next-generation Sequencing for Mitochondrial Disorders." *British Journal of Pharmacology Br J Pharmacol* 171.8 (2014): 1837-853.
11. Chen, Hong, Kun Qian, Zhongwei Du, Jingyuan Cao, Andrew Petersen, Huisheng Liu, Lisle W. Blackbourn, Cindytzu-Ling Huang, Anthony Errigo, Yingnan Yin, Jianfeng Lu, Melvin Ayala, and Su-Chun Zhang. "Modeling ALS with IPSCs Reveals That Mutant SOD1 Misregulates Neurofilament Balance in Motor Neurons." *Cell Stem Cell* 14.6 (2014): 796-809.

Back To Table of Contents

12. Davies, K. M., M. Strauss, B. Daum, J. H. Kief, H. D. Osiewacz, A. Rycovska, V. Zickermann, and W. Kuhlbrandt. "Macromolecular Organization of ATP Synthase and Complex I in Whole Mitochondria." *Proceedings of the National Academy of Sciences* 108.34 (2011): 14121-4126.
13. Dhara, Sujoy K., and Steven L. Stice. "Neural Differentiation of Human Embryonic Stem Cells." *Journal of Cellular Biochemistry J. Cell. Biochem.* 105.3 (2008 Oct): 633-40.
14. Dhara, Sujoy K., Kowser Hasneen, David W. Machacek, Nolan L. Boyd, Raj R. Rao, and Steven L. Stice. "Human Neural Progenitor Cells Derived from Embryonic Stem Cells in Feeder-free Cultures."*Differentiation* 76.5 (2008 May): 454-64.
15. Difrancesco, Jacopo C., J. Mark Cooper, Amanda Lam, Paul E. Hart, Lucio Tremolizzo, Carlo Ferrarese, and Antony H. Schapira. "MELAS Mitochondrial DNA Mutation A3243G Reduces Glutamate Transport in Cybrids Cell Lines." *Experimental Neurology* 212.1 (2008): 152-56.
16. Dimos, J. T., K. T. Rodolfa, K. K. Niakan, L. M. Weisenthal, H. Mitsumoto, W. Chung, G. F. Croft, G. Saphier, R. Leibel, R. Goland, H. Wichterle, C. E. Henderson, and K. Eggan. "Induced Pluripotent Stem Cells Generated from Patients with ALS Can Be Differentiated into Motor Neurons." *Science* 321.5893 (2008): 1218-221.
17. Ebner, Sabine, Roland Lang, Edith E. Mueller, Waltraud Eder, Michaela Oeller, Alexandra Moser, Josef Koller, Bernhard Paulweber, Johannes A. Mayr, Wolfgang Sperl, and Barbara Kofler. "Mitochondrial Haplogroups, Control Region Polymorphisms and Malignant Melanoma: A Study in Middle European Caucasians." *PLoS ONE* 6.12 (2011)
18. Efe, Jem A., Simon Hilcove, Janghwan Kim, Hongyan Zhou, Kunfu Ouyang, Gang Wang, Ju Chen, and Sheng Ding. "Conversion of Mouse Fibroblasts into Cardiomyocytes Using a Direct Reprogramming Strategy." *Nature Cell Biology Nat Cell Biol* 13.3 (2011): 215-22.
19. El-Hattab, Ayman W., and Fernando Scaglia. "Mitochondrial Cytopathies." *Cell Calcium* (2016).
20. Elkabetz, Y., G. Panagiotakos, G. Al Shamy, N. D. Socci, V. Tabar, and L. Studer. "Human ES Cell-derived Neural Rosettes Reveal a Functionally Distinct Early Neural Stem Cell Stage." *Genes & Development* 22.2 (2008): 152-65.
21. Estaquier, Jérome, François Vallette, Jean-Luc Vayssiere, and Bernard Mignotte. "The Mitochondrial Pathways of Apoptosis." *Advances in Experimental Medicine and Biology Advances in Mitochondrial Medicine* (2011): 157-83.
22. Finsterer, Josef. "Leigh and Leigh-Like Syndrome in Children and Adults." *Pediatric Neurology* 39.4 (2008): 223-35.
23. Friedman, Jonathan R., Arnaud Mourier, Justin Yamada, J. Michael Mccaffery, and Jodi Nunnari. "MICOS Coordinates with Respiratory Complexes and Lipids to Establish Mitochondrial Inner Membrane Architecture." *ELife* 4 (2015).
24. Ghosh, Soumitra S., Russell H. Swerdlow, Scott W. Miller, Brina Sheeman, W. Davis Parker, and Robert E. Davis. "Use of Cytoplasmic Hybrid Cell Lines for Elucidating the Role of Mitochondrial Dysfunction in Alzheimer's Disease and Parkinson's Disease." *Annals NY Acad Sci Annals of the New York Academy of Sciences* 893.1 OXIDATIVE/ENE (1999): 176-91.
25. Govatati, Suresh, Bulle Saradamma, Sravanthi Malempati, Divyamaanasa Dasi, Murali Krishna Thupurani, Narayana Nagesh, Sisinthy Shivaji, Manjula Bhanoori, Raghava Rao

Tamanam, Varadacharyulu Nallanchakravarthula, and Sreenivasa Rao Pasupuleti. "Association of Mitochondrial Displacement Loop Polymorphisms with Risk of Colorectal Cancer in South Indian Population." *Mitochondrial DNA Part A* (2016): 1-6.
26. Gray, M. W. "Mitochondrial Evolution." *Science* 283.5407 (1999): 1476-481.
27. Green, Douglas R., and Fabien Llambi. "Cell Death Signaling." *Cold Spring Harbor Perspectives in Biology Cold Spring Harb Perspect Biol* 7.12 (2015).
28. Hartzog, P. E., and B. D. Cain. "The Aleu207--arg Mutation in F1F0-ATP Synthase from Escherichia Coli. A Model for Human Mitochondrial Disease." *The Journal of Biological Chemistry* 268.17 (1993): 12250-2252.
29. Hatakeyama, Hideyuki, Ayako Katayama, Hirofumi Komaki, Ichizo Nishino, and Yu-Ichi Goto. "Molecular Pathomechanisms and Cell-type-specific Disease Phenotypes of MELAS Caused by Mutant Mitochondrial TRNATrp." *Acta Neuropathologica Communications Acta Neuropathol Commun* 3.1 (2015).
30. Hayashi, Teruo, Rosario Rizzuto, Gyorgy Hajnoczky, and Tsung-Ping Su. "MAM: More than Just a Housekeeper." *Trends in Cell Biology* 19.2 (2009): 81-88.
31. Iyer, S., E. Xiao, K. Alsayegh, N. Eroshenko, M. J. Riggs, J. P. Bennett, and R. R. Rao. "Mitochondrial Gene Replacement in Human Pluripotent Stem Cell-derived Neural Progenitors." *Gene Therapy Gene Ther* 19.5 (2011): 469-75.
32. Iyer, Shilpa, Khaled Alsayegh, Sheena Abraham, and Raj R. Rao. "Stem Cell-Based Models and Therapies for Neurodegenerative Diseases." *Crit Rev Biomed Eng Critical Reviews™ in Biomedical Engineering* 37.4-5 (2009): 321-53.
33. Johns, Donald R. "Paternal Transmission of Mitochondrial DNA Is (fortunately) Rare." *Annals of Neurology Ann Neurol.* 54.4 (2003): 422-24.
34. Kandola, K., A. Bowman, and M. A. Birch-Machin. "Oxidative Stress - a Key Emerging Impact Factor in Health, Ageing, Lifestyle and Aesthetics." *International Journal of Cosmetic Science Int J Cosmet Sci* 37 (2015): 1-8.
35. Karbowski, M., and R. J. Youle. "Dynamics of Mitochondrial Morphology in Healthy Cells and during Apoptosis." *Cell Death Differ Cell Death and Differentiation* 10.8 (2003): 870-80.
36. Katsetos, Christos D., Sirma Koutzaki, and Joseph J. Melvin. "Mitochondrial Dysfunction in Neuromuscular Disorders." *Seminars in Pediatric Neurology* 20.3 (2013): 202-15.
37. Keller, Gordon M. "In Vitro Differentiation of Embryonic Stem Cells." *Current Opinion in Cell Biology* 7.6 (1995): 862-69.
38. Keränen, Tapani, and Hanna Kuusisto. "NARP Syndrome and Adultonset Generalised Seizures." *Epileptic Discord* 8.3 (2006): 200-03.
39. Kerr, J. F R, A. H. Wyllie, and A. R. Currie. "Apoptosis: A Basic Biological Phenomenon with Wideranging Implications in Tissue Kinetics." *Br J Cancer British Journal of Cancer* 26.4 (1972): 239-57.
40. Kim, Janghwan, Rajesh Ambasudhan, and Sheng Ding. "Direct Lineage Reprogramming to Neural Cells." *Current Opinion in Neurobiology* 22.5 (2012): 778-84.
41. Kühlbrandt, Werner. "Structure and Function of Mitochondrial Membrane Protein Complexes." *BMC Biology BMC Biol* 13.1 (2015):

42. Kuznetsov, Andrey V., and Raimund Margreiter. "Heterogeneity of Mitochondria and Mitochondrial Function within Cells as Another Level of Mitochondrial Complexity." *IJMS International Journal of Molecular Sciences* 10.4 (2009): 1911-929.
43. Kuznetsov, Andrey V., Yves Usson, Xavier Leverve, and Raimund Margreiter. "Subcellular Heterogeneity of Mitochondrial Function and Dysfunction: Evidence Obtained by Confocal Imaging." *Molecular and Cellular Biochemistry Mol Cell Biochem* 256.1/2 (2004): 359-65.
44. Lay, Sui, Oana Sanislav, Sarah J. Annesley, and Paul R. Fisher. "Mitochondrial Stress Tests Using Seahorse Respirometry on Intact Dictyostelium Discoideum Cells." *Methods in Molecular Biology Chemotaxis* (2016): 41-61.
45. Li H. (2012) Exploring single-sample SNP and INDEL calling with whole-genome de novo assembly. Bioinformatics, 28, 1838-1844.
46. Li, Lin Z. "Imaging Mitochondrial Redox Potential and Its Possible Link to Tumor Metastatic Potential." *Journal of Bioenergetics and Biomembranes J Bioenerg Biomembr* 44.6 (2012): 645-53.
47. Li, Mingkun, Anna Schönberg, Michael Schaefer, Roland Schroeder, Ivane Nasidze, and Mark Stoneking. "Detecting Heteroplasmy from High-Throughput Sequencing of Complete Human Mitochondrial DNA Genomes." *The American Journal of Human Genetics* 87.2 (2010): 237-49.
48. Li, Peng, Deepak Nijhawan, Imawati Budihardjo, Srinivasa M. Srinivasula, Manzoor Ahmad, Emad S. Alnemri, and Xiaodong Wang. "Cytochrome C and DATP-Dependent Formation of Apaf-1/Caspase-9 Complex Initiates an Apoptotic Protease Cascade." *Cell* 91.4 (1997): 479-89.
49. Liou, C.-W., T.-K. Lin, J.-B. Chen, M.-M. Tiao, S.-W. Weng, S.-D. Chen, Y.-C. Chuang, J.-H. Chuang, and P.-W. Wang. "Association between a Common Mitochondrial DNA D-loop Polycytosine Variant and Alteration of Mitochondrial Copy Number in Human Peripheral Blood Cells." *Journal of Medical Genetics* 47.11 (2010): 723-28.
50. Luo, Yu, Alan Hoffer, Barry Hoffer, and Xin Qi. "Mitochondria: A Therapeutic Target for Parkinson's Disease?" *IJMS International Journal of Molecular Sciences* 16.9 (2015): 20704-0730.
51. Mandal, Pankaj K., and Derrick J. Rossi. "Reprogramming Human Fibroblasts to Pluripotency Using Modified MRNA." *Nat Protoc Nature Protocols* 8.3 (2013): 568-82.
52. Mazat, Jean-Pierre, Stéphane Ransac, Margit Heiske, Anne Devin, and Michel Rigoulet. "Mitochondrial Energetic Metabolism-some General Principles." *IUBMB Life* 65.3 (2013): 171-79.
53. Mccormack, James G., and Richard M. Denton. "Intracellular Calcium Ions and Intramitochondrial Ca in the Regulation of Energy Metabolism in Mammalian Tissues." *Proceedings of the Nutrition Society Proc. Nutr. Soc.* 49.01 (1990): 57-75.
54. Miller, F. J. "Precise Determination of Mitochondrial DNA Copy Number in Human Skeletal and Cardiac Muscle by a PCR-based Assay: Lack of Change of Copy Number with Age." *Nucleic Acids Research*31.11 (2003).
55. Nesbitt, V., R. D. S. Pitceathly, D. M. Turnbull, R. W. Taylor, M. G. Sweeney, E. E. Mudanohwo, S. Rahman, M. G. Hanna, and R. Mcfarland. "The UK MRC Mitochondrial Disease Patient Cohort Study: Clinical Phenotypes Associated with the M.3243AG

Mutation--implications for Diagnosis and Management." *Journal of Neurology, Neurosurgery & Psychiatry* 84.8 (2013): 936-38.
56. Neupert, Walter, and Johannes M. Herrmann. "Translocation of Proteins into Mitochondria." *Annu. Rev. Biochem. Annual Review of Biochemistry* 76.1 (2007): 723-49.
57. Onyango, Isaac G., Jameel Dennis, and Shaharyah M. Khan. "Mitochondrial Dysfunction in Alzheimer's Disease and the Rationale for Bioenergetics Based Therapies."*Aging and Disease A&D* 7.2 (2016): 201.
58. Pagliarini, D. J., and J. Rutter. "Hallmarks of a New Era in Mitochondrial Biochemistry." *Genes & Development* 27.24 (2013): 2615-627.
59. Paumard, Patrick, Jacques Vaillier, Bénédicte Coulary, Jacques Schaeffer, Vincent Soubannier, David M. Mueller, Daniel Brèthes, Jean-Paul Di Rago, and Jean Velours. "The ATP Synthase Is Involved in Generating Mitochondrial Cristae Morphology." *The EMBO Journal* 21.3 (2002): 221-30.
60. Perkins, G., C. Renken, M.e. Martone, S.j. Young, M. Ellisman, and T. Frey. "Electron Tomography of Neuronal Mitochondria: Three-Dimensional Structure and Organization of Cristae and Membrane Contacts." *Journal of Structural Biology* 119.3 (1997): 260-72.
61. Pfanner, Nikolaus, Martin Van Der Laan, Paolo Amati, Roderick A. Capaldi, Amy A. Caudy, Agnieszka Chacinska, Manjula Darshi, Markus Deckers, Suzanne Hoppins, Tateo Icho, Stefan Jakobs, Jianguo Ji, Vera Kozjak-Pavlovic, Chris Meisinger, Paul R. Odgren, Sang Ki Park, Peter Rehling, Andreas S. Reichert, M. Saeed Sheikh, Susan S. Taylor, Nobuo Tsuchida, Alexander M. Van Der Bliek, Ida J. Van Der Klei, Jonathan S. Weissman, Benedikt Westermann, Jiping Zha, Walter Neupert, and Jodi Nunnari. "Uniform Nomenclature for the Mitochondrial Contact Site and Cristae Organizing System." *J Cell Biol The Journal of Cell Biology* 204.7 (2014): 1083-086.
62. Poleganov, Marco Alexander, Sarah Eminli, Tim Beissert, Stephanie Herz, Jung-Il Moon, Johanna Goldmann, Arianne Beyer, Rosario Heck, Isabell Burkhart, Diana Barea Roldan, Özlem Türeci, Kevin Yi, Brad Hamilton, and Ugur Sahin. "Efficient Reprogramming of Human Fibroblasts and Blood-Derived Endothelial Progenitor Cells Using Nonmodified RNA for Reprogramming and Immune Evasion." *Human Gene Therapy* 26.11 (2015): 751-66.
63. Prigione, Alessandro, Björn Lichtner, Heiner Kuhl, Eduard A. Struys, Mirjam Wamelink, Hans Lehrach, Markus Ralser, Bernd Timmermann, and James Adjaye. "Human IPSCs Harbor Homoplasmic and Heteroplasmic Mitochondrial DNA Mutations While Maintaining HESC-Like Metabolic Reprogramming." *Stem Cells* (2011).
64. Raturi, Arun, and Thomas Simmen. "Where the Endoplasmic Reticulum and the Mitochondrion Tie the Knot: The Mitochondria-associated Membrane (MAM)." *Biochimica Et Biophysica Acta (BBA) - Molecular Cell Research* 1833.1 (2013): 213-24.
65. Riedl, Stefan J., and Yigong Shi. "Molecular Mechanisms of Caspase Regulation during Apoptosis." *Nature Reviews Molecular Cell Biology Nat Rev Mol Cell Biol* 5.11 (2004): 897-907.
66. Rizzuto, R. "Close Contacts with the Endoplasmic Reticulum as Determinants of Mitochondrial Ca2 Responses." *Science* 280.5370 (1998): 1763-766.

67. Rizzuto, Rosario, Diego De Stefani, Anna Raffaello, and Cristina Mammucari. "Mitochondria as Sensors and Regulators of Calcium Signalling." *Nature Reviews Molecular Cell Biology Nat Rev Mol Cell Biol* 13.9 (2012): 566-78.
68. Robinton, Daisy A., and George Q. Daley. "The Promise of Induced Pluripotent Stem Cells in Research and Therapy." *Nature* 481.7381 (2012): 295-305.
69. Russell, Oliver, and Doug Turnbull. "Mitochondrial DNA Disease—molecular Insights and Potential Routes to a Cure." *Experimental Cell Research* 325.1 (2014): 38-43.
70. Satoh, M. "Organization of Multiple Nucleoids and DNA Molecules in Mitochondria of a Human Cell." *Experimental Cell Research* 196.1 (1991): 137-40.
71. Saxton, W. M., and P. J. Hollenbeck. "The Axonal Transport of Mitochondria." *Journal of Cell Science* 125.9 (2012): 2095-104.
72. Schaefer, Andrew M., Robert W. Taylor, Douglass M. Turnbull, and Patrick F. Chinnery. "The Epidemiology of Mitochondrial Disorders—past, Present and Future."*Biochimica Et Biophysica Acta (BBA) - Bioenergetics* 1659.2-3 (2004): 115-20.
73. Schapira, Anthony Hv. "Mitochondrial Disease." *The Lancet* 368.9529 (2006): 70-82.
74. Schapira, Anthony Hv. "Mitochondrial Diseases." *The Lancet* 379.9828 (2012): 1825-834.
75. Schmidt, Oliver, Nikolaus Pfanner, and Chris Meisinger. "Mitochondrial Protein Import: From Proteomics to Functional Mechanisms." *Nature Reviews Molecular Cell Biology Nat Rev Mol Cell Biol* 11.9 (2010): 655-67.
76. Seelert, Holger, and Norbert A. Dencher. "ATP Synthase Superassemblies in Animals and Plants: Two or More Are Better." *Biochimica Et Biophysica Acta (BBA) - Bioenergetics*1807.9 (2011): 1185-197.
77. Sgarbi, Gianluca, Alessandra Baracca, Giorgio Lenaz, Lucia M. Valentino, Valerio Carelli, and Giancarlo Solaini. "Inefficient Coupling between Proton Transport and ATP Synthesis May Be the Pathogenic Mechanism for NARP and Leigh Syndrome Resulting from the T8993G Mutation in MtDNA." *Biochem. J. Biochemical Journal* 395.3 (2006): 493-500.
78. Shin, Soojung, Maisam Mitalipova, Scott Noggle, Deanne Tibbitts, Alison Venable, Raj Rao, and Steven L. Stice. "Long-Term Proliferation of Human Embryonic Stem Cell-Derived Neuroepithelial Cells Using Defined Adherent Culture Conditions." *Stem Cells* 24.1 (2006): 125-38.
79. Sun, Nuo, Richard J. Youle, and Toren Finkel. "The Mitochondrial Basis of Aging." *Molecular Cell* 61.5 (2016): 654-66.
80. Sutovsky, P. "Ubiquitinated Sperm Mitochondria, Selective Proteolysis, and the Regulation of Mitochondrial Inheritance in Mammalian Embryos." *Biology of Reproduction* 63.2 (2000): 582-90.
81. Taanman, Jan-Willem. "The Mitochondrial Genome: Structure, Transcription, Translation and Replication." *Biochimica Et Biophysica Acta (BBA) - Bioenergetics* 1410.2 (1999): 103-23.
82. Takahashi, Kazutoshi, and Shinya Yamanaka. "Induction of Pluripotent Stem Cells from Mouse Embryonic and Adult Fibroblast Cultures by Defined Factors." *Cell* 126.4 (2006): 663-76.

83. Takahashi, Kazutoshi, Keisuke Okita, Masato Nakagawa, and Shinya Yamanaka. "Induction of Pluripotent Stem Cells from Fibroblast Cultures." *Nat Protoc Nature Protocols* 2.12 (2007): 3081-089.
84. Tang, Sha, and Taosheng Huang. "Characterization of Mitochondrial DNA Heteroplasmy Using a Parallel Sequencing System." *BioTechniques Biotech.* 48.4 (2010): 287-96.
85. Tatuch, Y., J. Christodoulou, A. Feigenbaum, J. T. R. Clarke, J. Wherret, C. Smith, N. Rudd, R. Petrova-Benedict, and B. H. Robinson. "Heteroplasmic MtDNA Mutation (TG) at 8993 Can Cause Leigh Disease When the Percentage of Abnormal MtDNA Is High." *THe American Society of Human Genetics* (1992): 852-58.
86. Taylor, Robert W., and Doug M. Turnbull. "Mitochondrial DNA Mutations in Human Disease." *Nat Rev Genet Nature Reviews Genetics* 6.5 (2005): 389-402.
87. Thomson, J. A. "Embryonic Stem Cell Lines Derived from Human Blastocysts." *Science* 282.5391 (1998): 1145-147.
88. Thorvaldsdottir, H., J. T. Robinson, and J. P. Mesirov. "Integrative Genomics Viewer (IGV): High-performance Genomics Data Visualization and Exploration." *Briefings in Bioinformatics* 14.2 (2012): 178-92.
89. Tipirisetti, Nageswara Rao, Suresh Govatati, Priyanka Pullari, Sravanthi Malempati, Murali Krishna Thupurani, Shyam Perugu, Praveen Guruvaiah, Lakshmi Rao K, Raghunadha Rao Digumarti, Varadacharyulu Nallanchakravarthula, Manjula Bhanoori, and Vishnupriya Satti. "Mitochondrial Control Region Alterations and Breast Cancer Risk: A Study in South Indian Population." *PLoS ONE* 9.1 (2014)
90. Trimmer, Patricia A., and James P. Bennett. "The Cybrid Model of Sporadic Parkinson's Disease." *Experimental Neurology* 218.2 (2009): 320-25.
91. Wachsmuth, Manja, Alexander Hübner, Mingkun Li, Burkhard Madea, and Mark Stoneking. "Age-Related and Heteroplasmy-Related Variation in Human MtDNA Copy Number." *PLoS Genet PLOS Genetics*12.3 (2016).
92. Wallace, D. C. "Mitochondrial Diseases in Man and Mouse." *Science* 283.5407 (1999): 1482-488.
93. Warren, Luigi, Philip D. Manos, Tim Ahfeldt, Yuin-Han Loh, Hu Li, Frank Lau, Wataru Ebina, Pankaj K. Mandal, Zachary D. Smith, Alexander Meissner, George Q. Daley, Andrew S. Brack, James J. Collins, Chad Cowan, Thorsten M. Schlaeger, and Derrick J. Rossi. "Highly Efficient Reprogramming to Pluripotency and Directed Differentiation of Human Cells with Synthetic Modified MRNA." *Cell Stem Cell* 7.5 (2010): 618-30.
94. Wiedemann, N., A. E. Frazier, and N. Pfanner. "The Protein Import Machinery of Mitochondria." *Journal of Biological Chemistry* 279.15 (2004): 14473-4476.
95. Yang, D., Y. Oyaizu, H. Oyaizu, G. J. Olsen, and C. R. Woese. "Mitochondrial Origins." *Proceedings of the National Academy of Sciences* 82.13 (1985): 4443-447.
96. Yang, J. "Prevention of Apoptosis by Bcl-2: Release of Cytochrome C from Mitochondria Blocked." *Science* 275.5303 (1997): 1129-132.
97. Ylikallio, Emil, and Anu Suomalainen. "Mechanisms of Mitochondrial Diseases." *Annals of Medicine* 44.1 (2011): 41-59.
98. Yokota, Mutsumi, Hiroshi Shitara, Osamu Hashizume, Kaori Ishikawa, Kazuto Nakada, Rie Ishii, Choji Taya, Keizo Takenaga, Hiromichi Yonekawa, and Jun-Ichi Hayashi. "Generation of Trans-mitochondrial Mito-mice by the Introduction of a Pathogenic

G13997A MtDNA from Highly Metastatic Lung Carcinoma Cells." *FEBS Letters* 584.18 (2010): 3943-948.
99. Yoshida, Michiko, Shiho Kitaoka, Naohiro Egawa, Mayu Yamane, Ryunosuke Ikeda, Kayoko Tsukita, Naoki Amano, Akira Watanabe, Masafumi Morimoto, Jun Takahashi, Hajime Hosoi, Tatsutoshi Nakahata, Haruhisa Inoue, and Megumu K. Saito. "Modeling the Early Phenotype at the Neuromuscular Junction of Spinal Muscular Atrophy Using Patient-Derived IPSCs."*Stem Cell Reports* 4.4 (2015): 561-6
100. Zhang, Jin, Zhi-Xia Zhang, Peng-Chen Du, Wei Zhou, Su-Dong Wu, Qi-Ling Wang, Cao Chen, Qi Shi, Chen Chen, Chen Gao, Chan Tian, and Xiao-Ping Dong. "Analyses of the Mitochondrial Mutations in the Chinese Patients with Sporadic Creutzfeldt–Jakob Disease." *Eur J Hum Genet European Journal of Human Genetics* 23.1 (2014): 86-91.

APPENDIX

Appendix i: DNA mini kit protocol and mini-preparation ATP-Dependent DNase protocol

Mini kit protocol

1. Centrifuge thawed cell pellet for 5 minutes at 300 x g in a 1.5mL microcentrifuge tube.
2. Remove the supernatant completely and discard without disturbing the cell pellet.
3. Resuspend the cell pellet in 200 µL of phosphate buffered saline (PBS).
4. Add 20 µL of proteinase K.
5. Add 200 µL of buffer AL. Mix by pulse-vortexing for 15 seconds.
6. Incubate solution at 56°C for 10 minutes
7. Centrifuge to remove condensation from the lid.
8. Add 200 µL of 100% ethanol, and pulse-vortex for 15 seconds. Centrifuge to remove drops from the lid.
9. Apply mixture to QIAamp Mini spin column, and centrifuge at 6,000 x g for 1 minute.
10. Discard the filtrate, and place the spin column in a new collecting tube.
11. Add 500 µL of AW1 buffer to the spin column, and centrifuge at 6,000 x g for 1 minute.
12. Discard the filtrate, and place the spin column in a new collecting tube.
13. Add 500 µL of AW2 buffer to the spin column, and centrifuge at full speed (approximately 20,000 x g) for 3 minutes.
14. Discard the filtrate, and centrifuge again at full speed for 1 minute.
15. Place the spin column in a clean 1.5 mL microcentrifuge tube, and add 80 µL of nuclease free water. Incubate for 5 minutes.

16. Elute by centrifuging at 6,000 x g for 1 min.

Mini-preparation ATP-Dependent DNase protocol

Reaction Mixture	Amount (µL)
Nuclease free H_2O with total DNA	42
25 mM ATP	2
10X Reaction Buffer	5
Plasmid-Safe DNase (10U)	1
Total volume	**50**

1. Incubate the reaction mixture for 30 minutes at 37°C.
2. Inactivate DNase by incubating at 70°C.

Appendix ii: UltraClean 15 DNA Purification protocol and gel protocols

UltraClean 15 DNA purification protocol

Purifying DNA from a solution

1. Determine DNA solution volume (51 µL).
2. Add 3 volumes of ULTRA SALT (153 µL) and mix well.
3. Resuspend ULTRA BIND by vortexing for 1 minute or until homogenous.
4. Add ULTRA BIND. 5 µL plus 1 µL per µg of DNA you expect to recover (6 µL).
5. Incubate for 5 minutes at room temperature. Flick the tube, or invert the tube several time to insure proper mixing.
6. Centrifuge for 5 seconds, and discard the supernatant.

7. Let the pellet soak in 1 ml of ULTRA WASH/ETHANOL for 5 minutes. Do not vortex DNA larger than 15 kb to avoid shearling.
8. Centrifuge for 5 seconds, and discard supernatant.
9. Centrifuge for 5 seconds again, and remove all traces of the ULTRA WASH/ETHANOL.
10. Resuspend the pellet in 30 µL of nuclease free H_2O by gently pipetting.
11. Incubate for 5 minutes at room temperature.
12. Centrifuge for 1 minute.
13. Remove supernatant and transfer to a new clean 1.5 mL microcentrifuge tube.

Purifying DNA from a TBE buffered agarose gel

1. Determine weight of agarose gel band slice.
2. Add ½ volume of ULTRA MELT and 4.5 volumes of ULTRA SALT, and mix well.
3. Incubate at 55°C for approximately 5 minutes, or until gel is completely melted.
4. Follow steps 3-13 from the above protocol on purifying DNA from solution.

0.8% agarose gel preparation

1. Dissolve 1.4g of ultra-pure agarose in 175 ml of TBE buffer. Heat until agarose dissolves completely into solution. Let the solution cool to approximately 50°C.
2. Add 10.5 µL of ethidium bromide and stir under exhaust hood.
3. Pour the gel solution into a gel with the appropriate size gel comb in place. Let the solution cool.
4. Once the gel has solidified, pull the comb out without breaking the gel.

5. Mix 20 µL of cleaned up mtDNA with 3.33 µL of loading dye, and load the mix into the wells.
6. Load an appropriate gel ladder. Run the gel at 30 V for 8-10 hours. Low voltage run to avoid smearing the large 16 kb band.
7. Use the gel dock reader to extract the band.

2.0% agarose gel preparation

1. Dissolve 2g of ultra-pure agarose in 100 ml of TBE buffer. Heat until agarose dissolves completely into solution. Let the solution cool to approximately 50°C.
2. Add 6 µL of ethidium bromide and stir under exhaust hood.
3. Pour the gel solution into a gel with the appropriate size gel comb in place. Let the solution cool.
4. Once the gel has solidified, pull the comb out without breaking the gel.
5. Mix 10 µL of PCR amplified product with 1.67 µL of loading dye, and load the mix into the wells.
6. Load an appropriate gel ladder. Run the gel at 80 V for 1.5 hours.
7. Use the gel dock reader to record the size of the PCR products.

0.8% agarose gel results

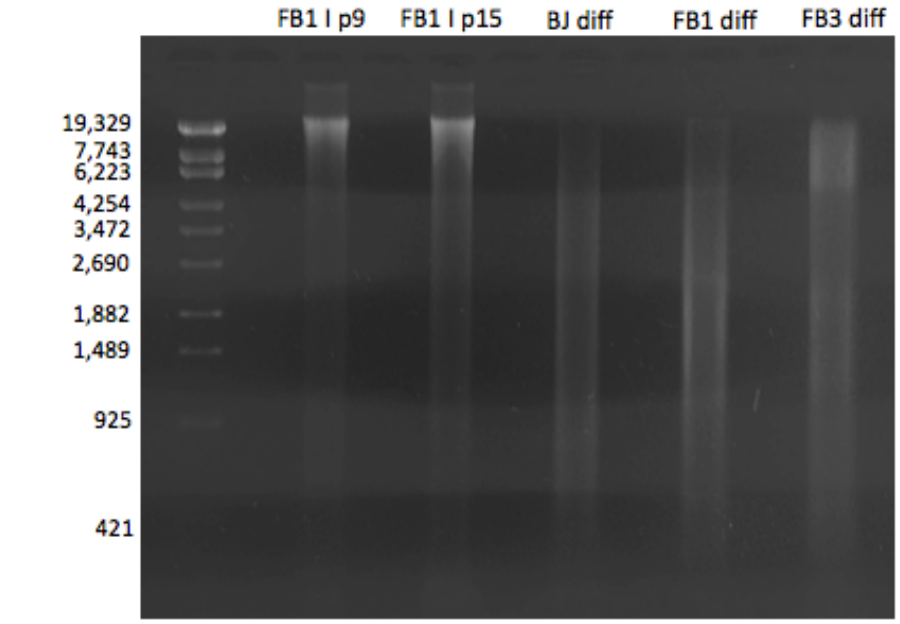

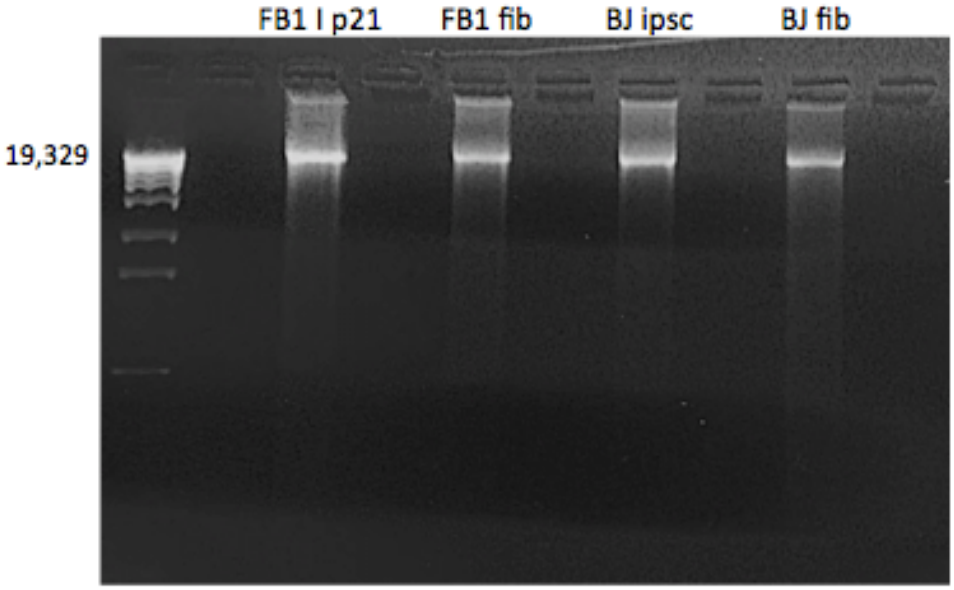

λ EcoT14i was used as a reference (Clontech, Mountain View, CA, USA)

2.0 % agarose gel results

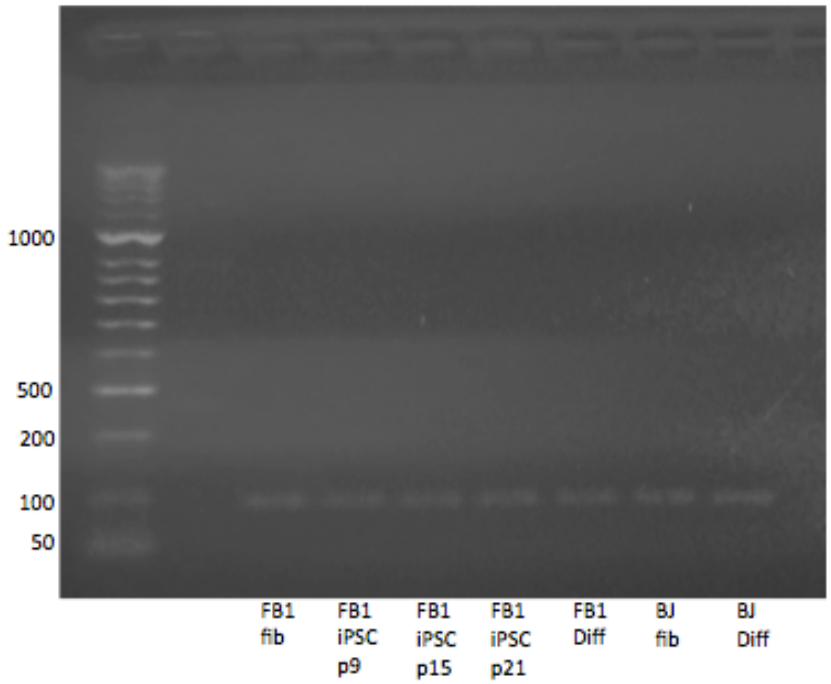

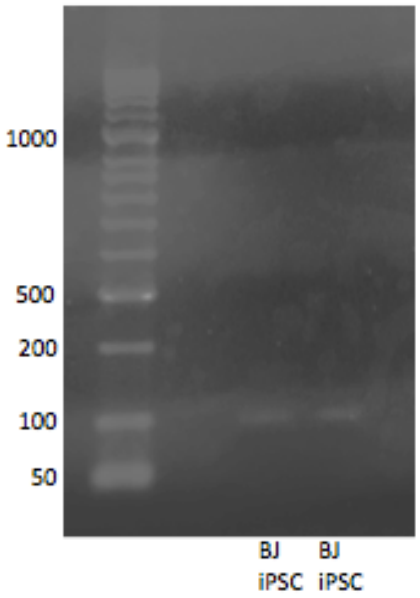

Hyperladder ii was used as a reference (Bioline, Taunton, MA, USA).

Appendix iii: NanoDrop results

NanoDrop concentration results after gel extraction

Sample Name	Concentration (ng/µL)
H9 p54	73.1
BJ FB p13	58.7
BJ iPSC p21	281.1
BJ Diff p24	35.6
FB1 p7	125.1
FB1 iPSC p9	79.0
FB1 iPSC p15	24.6
FB1 iPSC p21	44.1
FB1 Diff p24	31.7

NanoDrop concentration results after PCR amplification

Sample Name	Concentration (ng/µL)
H9 p54	88.3
BJ FB p13	62.5
BJ iPSC p21	62.7
BJ Diff p24	35.3
FB1 p7	128.8
FB1 iPSC p9	104.7
FB1 iPSC p15	38.6
FB1 iPSC p21	34.3
FB1 Diff p24	62.5

Appendix iv: PCR protocol and cycle information

PCR Reaction Setup	Stock Conc.	Volume per 50 µl Rxn	Final Conc.
10x PCR buffer	10	5	1
dNTP mixture	2.5	4	0.2
10uM Forward primer	10	1	0.2
10uM Reverse primer	10	1	0.2
Takara Taq	250	0.25	1.25
dd H20		38.25	
0.5 ng/50µl DNA	1	0.5	7.5
Total volume		**50**	

Cycling Steps	Temperatures and Times	Cycles
Denaturation	30 sec at 94°C	25
Annealing	30 sec at 55°C	
Extension	30 sec at 72°C	
Final Extension	2 min at 72°C	1

Appendix v: Cycle sequencing reaction and precipitation protocol

Cycle sequencing reaction for standard quarter reaction

Sequencing Reaction Setup	Amount
Big Dye	2 µl
Primer	X µl 3.2 pmol
Sequencing buff (5X)	1 µl
dd H20	X µl
DNA	X µl 60-100 ng
Total volume	**10**

Precipitation Protocol

1. Prepare 3 µl sodium acetate anhydrous (3M pH 4.6), 62.5 µl Ethanol (100 %), 14.5 µl water.
2. Add 10 µl of water to make the sequencing samples up to 20 µl.
3. Mix the sodium acetate anhydrous and ethanol with each sequencing sample.
4. Centrifuge for 30 minutes.
5. Remove the supernatant and add 250 µl of 70% ethanol.
6. Centrifuge for 3-5 minutes.
7. Remove supernatant and repeat 70% ethanol wash.
8. Remove supernatant completely.
9. Dry samples to remove ethanol.

Appendix vi: Variant Calling Files filter settings

In order to be included, sequences must be:

1. SNP posterior probability higher than 0.95
2. Number of variant reads greater than 3
3. Variant read ratio greater than 0.1
4. All variants are in a single strand direction
5. Total coverage must be greater than 30
6. Total coverage must be less than 100,000

VITA

John Patrick Galdun III was born on February 14, 1991, in Pittsburgh, Pennsylvania, and is an American citizen. Patrick graduated from the Webb School of Knoxville, Knoxville, Tennessee in 2009. In 2013, he received his Bachelors of Science in Microbiology from the University of Georgia in Athens, Georgia. Since 2014, Patrick has been pursuing his Masters of Science in Physiology and Biophysics at Virginia Commonwealth University in Richmond, Virginia. Patrick's future plans are to pursue a career in healthcare.

Back To Table of Contents